

ROLE OF Ca^{2+} IN SERS: SURFACE Ag^+ FORMATION AND ANION ADSORPTION - A MECHANISTIC APPROACH

GEORGIANA ION, ALEXANDRA M. CHIRIAC, RALUCA A. CICEO-LUCACEL,
VLAD MOISOIU, ANDREI STEFANCU, STEFANIA D. IANCU*, NICOLAE LEOPOLD*

Faculty of Physics, Babeş-Bolyai University, Kogalniceanu 1, 400084 Cluj-Napoca, Romania

*Corresponding authors: stefania.iancu@ubbcluj.ro; nicolae.leopold@ubbcluj.ro

Received

Abstract. The activation of surface-enhanced Raman scattering (SERS) signals is commonly attributed to nanoparticle aggregation, while the contribution of analyte adsorption is often overlooked. Here, we show that silver nanoparticles act as nanoelectrodes, with their electrochemical potential (Fermi level) tuned *in situ* by atomic ions. This modulation of surface potential dictates the selective adsorption of anionic and cationic analytes, thereby enabling controlled SERS activation. Specifically, the addition of Ca^{2+} to colloidal AgNPs depletes electrons from the metal and promotes the formation of surface Ag^+ , as confirmed by X-ray photoelectron spectroscopy. In our model, Ca^{2+} addition increases the ionic strength of the medium, reducing the Debye radius around the nanoparticles. Under these conditions, ion transport is governed by diffusion rather than migration. Because H^+ diffuses faster than OH^- , localized acidification at the nanoparticle surface occurs, which further enhances electron depletion, drives surface Ag^+ formation, and lowers the Fermi level. This favors adsorption of anionic species such as citrate, thereby activating their SERS signal. Conversely, Cl^- adsorption induces partial charge transfer to the nanoparticle, resulting in a Fermi level upshift. This more negative electrochemical potential promotes the adsorption and ultrasensitive SERS detection of cationic analytes such as Nile Blue (10^{-8} M). Overall, these findings demonstrate that SERS is switched on when analytes adsorb to the metal surface, where the localized electromagnetic near field is maximized.

Key words: electrochemical potential, surface Ag^+ , XPS.

1. INTRODUCTION

The role of Ag^+ sites on silver electrodes in enabling surface-enhanced Raman scattering (SERS) of species that form Ag^+ -complexes was recognized by Pettinger in electrochemical SERS studies in the early 1980s [1]. Weakly water-

soluble Ag^+ -complexes, such as those formed with pyridine and halide ions, tend to remain adsorbed on the silver surface. In contrast, highly water-soluble Ag^+ -complexes, such as those with thiosulfate ($\text{S}_2\text{O}_3^{2-}$), readily dissolve into the aqueous phase, detaching from the surface. Consequently, SERS spectra of pyridine and halide ions were only observed in the presence of surface Ag^+ . Notably, these spectra disappear after rinsing the silver electrode with a thiosulfate solution—a photographic fixing agent—which selectively removes surface Ag^+ while leaving metallic silver (Ag^0) intact [1].

During the same period, Blatchford *et al.* investigated the role of the electrochemical potential (equivalent to the Fermi level) of colloidal silver nanoparticles (AgNPs) for citrate SERS detection [2]. Depletion of metal electrons from the surface layer of AgNPs gives rise to several complex effects that critically influence whether SERS is observed or not. These include alterations in the optical properties of the nanoparticles, molecular adsorption and desorption, and nanoparticle aggregation. Although Blatchford *et al.* observed that the SERS spectrum of anionic citrate appeared only when the nanoparticles possessed positive potentials, they attributed the appearance and disappearance of the spectra primarily to aggregation–disaggregation processes. In contrast, we emphasize a potential-dependent adsorption–desorption mechanism: adsorption of citrate is favored at positive surface potentials, whereas desorption dominates at negative potentials, leading to the loss of the SERS response.

On the other hand, inducing nanoparticle aggregation through relatively high concentrations of Cl^- ($>10^{-3}$ M) or Mg^{2+} ($>5\times 10^{-4}$ M) [3] has become a standard practice in SERS methodology, with the goal of generating electromagnetic hot spots in the gaps between particles. However, the explanation of SERS activation primarily through aggregation has been a source of controversy, as it fails to account for the selectivity observed in SERS. Moreover, this framework does not explain why surfactants such as citrate or chloride, or the water solvent, exhibit no detectable Raman enhancement in the hotspots, even though their concentrations exceed that of the analyte by several orders of magnitude [4].

Over the past seven years, our studies [5-11] have provided compelling evidence for the crucial role of analyte adsorption onto nanoparticle surfaces prior to aggregation. Moreover, this adsorption is selective for either cationic or anionic analytes. For instance, halide ions (Cl^- , Br^- , I^-) at concentrations below 10^{-3} M promote the selective adsorption of cationic species. In contrast, the addition of metal cations such as Ca^{2+} , Mg^{2+} , Pb^{2+} , or Al^{3+} (up to 5×10^{-4} M) facilitates the selective adsorption - and subsequent SERS detection - of anionic species [7].

In our initial work [8], we attributed this effect to the electrostatic interaction of atomic cations with anionic species, hypothesizing that the cations assume a bridging role. More recently, we recognized that both anionic and cationic atomic

ions play a unified role in modulating the electrochemical potential of the nanoparticle surface [5, 11]. Halide ions adsorb onto AgNPs and raise the surface Fermi level through partial charge transfer [6, 12-13]. The magnitude of this upshift is halide-dependent ($\text{Cl}^- < \text{Br}^- < \text{I}^-$) and can reach ~ 0.3 eV [6]. This shift of the surface electrochemical potential toward more negative values enhances the affinity for cationic analytes and enables their ultrasensitive SERS detection. As a result, in colloids containing residual Cl^- from synthesis, the SERS spectrum of cationic dyes can be recorded spontaneously at concentrations as low as 10^{-9} M [8]. In contrast, citrate-reduced colloids require the addition of Cl^- to achieve comparable sensitivity for cationic dye detection [8-9].

Conversely, the adsorption of anionic species involves an opposite mechanism - lowering of the Fermi level through electron depletion. The addition of Ca^{2+} to the colloidal silver suspension increases the ionic strength, thereby reducing the Debye length and causing a more rapid decay of the electric field around the nanoparticles associated with the surface double-layer. As a result, ion transport is governed predominantly by diffusion rather than migration in the electric field gradient. Because H^+ diffuses more rapidly than OH^- , protons preferentially accumulate at the nanoparticle interface, leading to localized surface acidification. This effect is evidenced by the Ag^+ component in the X-ray photoelectron spectroscopy (XPS) spectrum of the Ca^{2+} -supplemented colloid. The acidified environment promotes the generation of Ag^+ sites through depletion of metal electrons, thereby lowering the surface electron density. The associated reduction of the Fermi level enhances the adsorption affinity for anionic species, thereby facilitating their SERS activation.

2. EXPERIMENTAL

2.1. SILVER NANOPARTICLES (AgNPs) SYNTHESIS

All reagents were of analytical grade. Citrate-reduced silver nanoparticles (cit-AgNPs) were synthesized using the Lee–Meisel method [14]. Briefly, 17 mg of silver nitrate were dissolved in 98 mL of ultrapure water (Millipore Direct-Q3 UV) under continuous magnetic stirring. The solution was heated on a hot plate set to 200 °C until it reached boiling and was maintained at the boiling point for an additional 1–2 minutes. The hot plate temperature was then reduced to 150 °C. Subsequently, 2 mL of freshly prepared 1% (w/v) trisodium citrate solution were added dropwise using a 2 mL syringe fitted with a needle. After citrate addition, the mixture was maintained at boiling under stirring for further 30 minutes.

The fivefold concentrated colloidal silver solution was obtained by centrifugation at $7300\times g$ for 5 min at 25 °C. Following centrifugation, from the initial 2 mL volume, 1.6 mL of the supernatant was carefully removed. The resulting concentrated cit-AgNPs were then used for subsequent measurements. For experiments with Ca^{2+} supplementation, $\text{Ca}(\text{NO}_3)_2$ was added to a final concentration of 3×10^{-4} M.

2.2. X-RAY PHOTOELECTRON SPECTROSCOPY (XPS) ANALYSIS

XPS measurements were performed using a SPECS PHOIBOS 150 MCD system (Surface Nano Analysis GmbH, Berlin, Germany) equipped with a monochromatic Al $K\alpha$ X-ray source (250 W, $h\nu=1486.6$ eV), a hemispherical analyzer, and a multichannel detector. Binding energies were charge-referenced to the C1s photoelectron peak at 284.6 eV. Survey spectra were acquired with a pass energy of 60 eV over a binding energy range of 0–1200 eV. High-resolution spectra were collected at a pass energy of 20 eV.

Spectral deconvolution was performed using CasaXPS (Casa Software Ltd., Teignmouth, UK), applying a Shirley-type background. Peak positions and full widths at half maximum (FWHM) were determined using a GL(30) mixed line shape, combining Gaussian and Lorentzian functions.

For sample preparation, 50 μL of the colloidal suspension was deposited onto a carbon tape support. Measurements were carried out at room temperature under ultra-high vacuum (10^{-9} - 10^{-10} mbar), with charge neutralization applied to all samples to prevent charging effects.

2.3. SURFACE-ENHANCED RAMAN SCATTERING (SERS) AND UV-VIS MEASUREMENTS

SERS spectra were recorded using an InVia Raman spectrometer (Renishaw) coupled to a Leica microscope. A 10 μL aliquot of the sample was placed on a microscope slide covered with aluminium foil. The 532 nm excitation laser was focused through a $5\times$ objective, and each spectrum was obtained by averaging three acquisitions with an exposure time of 5 s per acquisition.

UV-Vis spectra were recorded using a Jasco V-630 spectrophotometer equipped with a quartz cuvette (1 cm path length). For each measurement, 90 μL of the cit-AgNP suspension was combined with either 10 μL of a $\text{Ca}(\text{NO}_3)_2$ solution to obtain a final Ca^{2+} concentration of 3×10^{-4} M, or with 10 μL of ultrapure water for the control. The mixtures were subsequently diluted tenfold prior to spectral acquisition.

For experiments under oxygen-free conditions, the colloidal solution was purged with argon. In a 2 mL vial, cit-AgNPs were added, and a thin tube connected to an argon cylinder was inserted into the vial. After argon purging, the cit-AgNPs were

supplemented with Ca²⁺ ions to a final concentration of 3×10^{-4} M. During the purging process, a slight darkening of the solution was observed.

3. RESULTS AND DISCUSSION

3.1. Ca²⁺-INDUCED SURFACE ACIDIFICATION AND OXIDATION OF SILVER NANOPARTICLES (AgNPs)

Surface-enhanced Raman scattering (SERS) and X-ray photoelectron spectroscopy (XPS) can be considered complementary methods: SERS probes molecules adsorbed on the metal surface, whereas XPS examines the surface itself with electron-level precision.

Colloidal AgNPs synthesized via citrate reduction using the Lee–Meisel method consist exclusively of fully reduced silver, as confirmed by XPS. The XPS spectrum in Fig. 1A is accurately fitted by a single component corresponding to metallic silver (Ag⁰). The colloid was concentrated fivefold, as described in the Experimental section, to increase the silver mass per unit volume, thereby enhancing the signal-to-noise ratio and ensuring optimal spectral quality for XPS analysis.

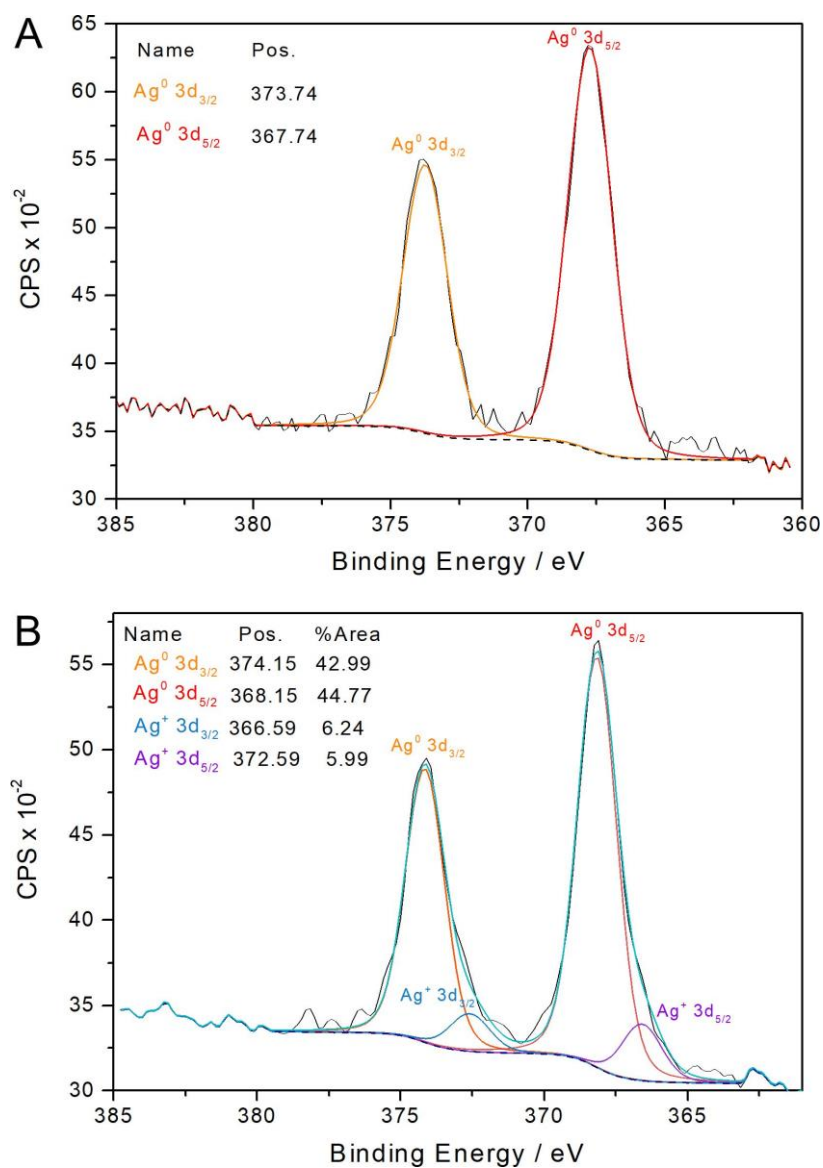


Fig. 1 – X-ray photoelectron spectroscopy (XPS) spectra of the Ag3d binding energy region for (A) citrate-reduced silver nanoparticles (cit-AgNPs) and (B) cit-AgNPs modified with Ca²⁺ (3×10^{-4} M).

The addition of Ca²⁺ to the colloidal solution promotes anionic citrate adsorption and activates its SERS spectrum. Before discussing this effect in detail, we first examine the processes occurring at the silver surface upon the addition of Ca(NO₃)₂ (final concentration 3×10^{-4} M) to cit-AgNPs. As shown in Fig. 1B, the Ag3d XPS

binding energy region of silver after Ca^{2+} addition can no longer be adequately fitted with a single component; instead, a contribution from Ag^+ becomes evident, appearing as a shoulder at lower binding energies. The deconvoluted Ag^+ component accounts for 12% of the total area of the $\text{Ag}3d$ doublet. Similarly, in our recent work [5], we observed that adding 5×10^{-4} M Ca^{2+} to a citrate-reduced colloid led to the appearance of nearly 50% Ag^+ species.

At first sight, the emergence of surface Ag^+ after Ca^{2+} addition appears counterintuitive, since the oxidation of Ag^0 to Ag^+ requires a suitable oxidizing agent. The model we propose for the generation of surface Ag^+ builds on our previous observation at acidic pH, where we found that at pH 4 citrate spontaneously adsorbs onto colloidal silver [7]. Considering this, the appearance of surface Ag^+ in the presence of Ca^{2+} can be rationalized by a mechanism whereby Ca^{2+} promotes surface acidification, which in turn facilitates the oxidation of silver atoms at the nanoparticle surface - a mechanism further detailed in the subsequent section.

To understand how surface acidification occurs at nanoparticle interfaces, it is useful to first consider the study of Stepan *et al.* [15], who calculated the near-surface ion distribution around spherical nanoparticles by solving the diffusion equation. The pH at the nanoparticle surface was obtained from the Nernst equation. Their results showed that a steep pH gradient forms close to the nanoparticle surface, and this effect becomes more pronounced as the nanoparticle size decreases. The difference in diffusion coefficients - H^+ diffusing $\sim 1.8 \times$ faster than OH^- - tilts the balance of flux, so that protons accumulate more readily near the nanoparticle surface, producing sharp local pH gradients. Thus, a localized acidification arises: H^+ ions tend to accumulate at the nanoparticle interface, where they are transiently trapped.

However, in the as-synthesized cit-AgNPs, only metallic Ag^0 was detected, as confirmed by the XPS spectrum in Fig. 1A, with no indication of surface acidification sufficient to locally lower the pH and promote Ag^+ formation. Stepan *et al.* employed a simplified model that accounted solely for ion diffusion while neglecting migration - the contribution of ion motion under an electric field gradient - which limits the model's ability to fully capture the surface processes involved. We hypothesize that the electric field gradient of the unmodified nanoparticle double layer limits the preferential transport and accumulation of protons at the nanoparticle. In contrast, upon Ca^{2+} addition, the XPS spectrum (Fig. 1B) shows clear evidence of surface Ag^+ formation, which we attribute to silver oxidation driven by localized surface acidification.

We advance this understanding by proposing a mechanism that explains how surface acidification emerges under these conditions: the introduction of Ca^{2+} into the silver colloid increases the ionic strength and decreases the Debye length around the nanoparticles, thereby compacting the electric double layer, as schematically illustrated in Fig. 2.

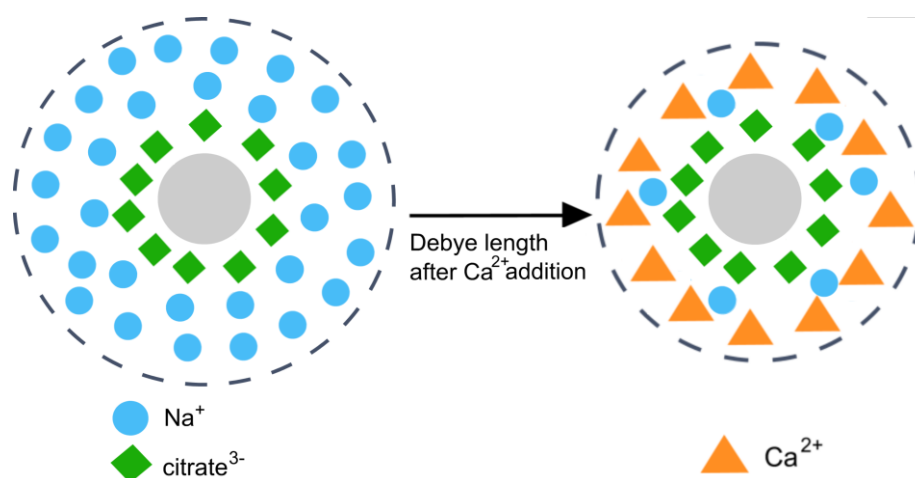


Fig. 2 – Schematic illustration showing the reduction of the Debye radius around a citrate-stabilized silver nanoparticle upon the addition of Ca^{2+} ions.

The reduction of the double layer length suppresses migration effects, rendering diffusion-dominated transport the prevailing mechanism and thereby validating the assumption of Stepan et al. Under these conditions, the higher diffusion coefficient of H^+ ($9.31 \times 10^{-9} \text{ m}^2 \cdot \text{s}^{-1}$) relative to OH^- ($5.27 \times 10^{-9} \text{ m}^2 \cdot \text{s}^{-1}$) drives proton accumulation at the nanoparticle interface, leading to localized acidification of the AgNP surface [15]. Once such a nano-environment is established, the acidic conditions promote the oxidation of metallic silver atoms at the nanoparticle surface ($\text{Ag} \rightleftharpoons \text{Ag}^+ + \text{e}^-$). This oxidation is facilitated by species naturally present in solution, including protons ($2\text{H}^+ + 2\text{e}^- \rightleftharpoons \text{H}_2$) and dissolved oxygen ($\text{O}_2 + 4\text{H}^+ + 4\text{e}^- \rightleftharpoons 2\text{H}_2\text{O}$) [16]. As a result, the XPS spectrum in Fig. 1B revealed distinct signals attributed to Ag^+ species at the nanoparticle surface, providing direct spectroscopic evidence that the interplay between localized acidification and redox-active solution species drives partial surface oxidation of the colloidal AgNP surface.

3.2. SURFACE ELECTRON DEPLETION LOWERS THE FERMI LEVEL AND PROMOTES ANIONIC CITRATE ADSORPTION

The formation of surface Ag^+ upon Ca^{2+} supplementation can also be inferred indirectly from the activation of the SERS spectrum of anionic citrate. When light excites surface plasmons on a metal nanoparticle, the oscillating metal electrons generate localized electromagnetic fields confined to the immediate vicinity of the nanoparticle surface. This near field, enhanced by several orders of magnitude (relative to the incident electromagnetic field), greatly amplifies the Raman scattering of molecules located within it. Accordingly, analytes must be located within the near-field region to experience maximal scattering enhancement.

The SERS spectrum of the fivefold-concentrated colloidal solution shows no detectable signal, displaying only weak Raman bands of water (Fig. 3A). The blank spectrum reflects the absence of analyte adsorption within the near-field region.

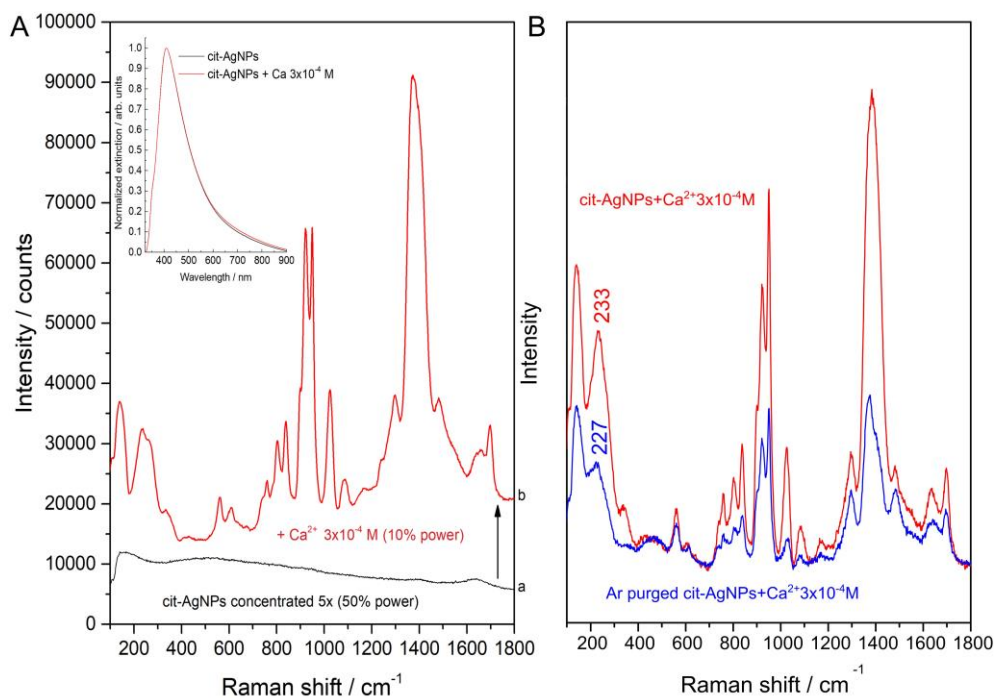


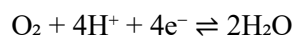
Fig. 3 – (A) (a) Blank spectrum of a fivefold concentrated silver colloid obtained by citrate reduction (cit-AgNPs) showing no detectable SERS bands. (b) Spectrum of the same colloid after the addition of 3×10^{-4} M Ca^{2+} , revealing the characteristic SERS peaks of citrate. Spectral intensities are presented as recorded, without preprocessing. Inset: Extinction spectra of cit-AgNPs (black line) and cit-AgNPs with 3×10^{-4} M Ca^{2+} (red line). (B) (red line) Citrate SERS spectrum recorded after supplementation of cit-AgNPs with 3×10^{-4} M Ca^{2+} . (blue line) Citrate SERS spectrum of a cit-AgNP colloid purged with argon prior to Ca^{2+} addition to remove dissolved oxygen.

The addition of Ca^{2+} (3×10^{-4} M) to cit-AgNPs shifts the surface potential toward positive values, thereby creating an electrochemical environment favorable for citrate adsorption. This leads to the appearance of the SERS spectrum of citrate (Fig. 3A). To emphasize that adsorption, rather than nanoparticle aggregation, accounts for the appearance of the citrate SERS spectrum, Fig. 3A shows as an inset the extinction spectra of cit-AgNPs and cit-AgNPs supplemented with 3×10^{-4} M Ca^{2+} . The extinction spectra were normalized to unity to highlight potential differences in spectral shape. The overlapping spectra before and after Ca^{2+} addition demonstrate that, at this concentration, Ca^{2+} does not induce nanoparticle aggregation.

Instead, as previously discussed, the role of Ca^{2+} is to increase the ionic strength, thereby reducing the Debye length, screening migration effects, and promoting diffusion-dominated ion transport. This process favors the accumulation of H^+ at the nanoparticle surface, followed by Ag oxidation. Electron depletion associated with surface Ag^+ formation lowers the Fermi level, effectively shifting the electrochemical potential toward more positive values. The resulting positive surface potential promotes the adsorption of anionic citrate onto the metal surface, thereby activating the citrate SERS spectrum (Fig. 3A).

Since no SERS bands which could result from the direct interaction of Ca^{2+} with the Ag surface were observed, we infer that Ca^{2+} does not adsorb directly to the Ag surface, as initially assumed [8]. Instead, it reduces the Debye radius, leading to surface acidification that drives partial oxidation of silver.

Our experimental findings further indicate that this oxidative pathway is coupled to electron transfer from AgNPs to dissolved molecular oxygen, which serves as the terminal electron acceptor according to the reaction:



The involvement of this pathway is evidenced in Fig. 3B, where the SERS spectrum of citrate is shown after supplementation of cit-AgNPs with 3×10^{-4} M Ca^{2+} . In a complementary control experiment, cit-AgNPs were first purged with argon to remove dissolved oxygen prior to Ca^{2+} addition. As shown in Fig. 3B, oxygen depletion resulted in a markedly attenuated citrate SERS response, thereby confirming that molecular oxygen is essential for driving surface Ag^+ generation.

Taken together, these results show that Ca^{2+} acts indirectly by modulating the electrostatic environment to induce proton-driven surface acidification, while molecular oxygen acts as the redox sink driving Ag^+ formation and Fermi level lowering, thereby creating favorable conditions for citrate adsorption and SERS activation.

3.3. ELECTROCHEMICAL POTENTIAL DEPENDENT SELECTIVITY FOR ANIONIC AND CATIONIC ANALYTES ADSORPTION

We demonstrate that AgNPs behave as nanoelectrodes, with their Fermi level modulated *in situ* by atomic ions through electron depletion or donation. The resulting surface electrochemical potential dictates the selective adsorption of anionic or cationic species, subsequently enabling their SERS activation.

Nile Blue (10^{-8} M) was selected as a representative cationic analyte, while citrate - originating from the nanoparticle synthesis and present in the colloidal solution at 10^{-3} M, served as the anionic analyte. Fig. 4 shows the effect of nanoparticle electrochemical potential, tuned *in situ* by the addition of Ca^{2+} and Cl^- ions, on the SERS spectra of citrate and Nile Blue.

The intrinsic electrochemical potential of as-synthesized cit-AgNPs does not favor adsorption of either citrate (10^{-3} M) or Nile Blue (10^{-8} M). Accordingly, the spectrum of 10^{-8} M Nile Blue in cit-AgNPs shows no detectable features apart from the Raman bands of water (Fig. 4A, spectrum a).

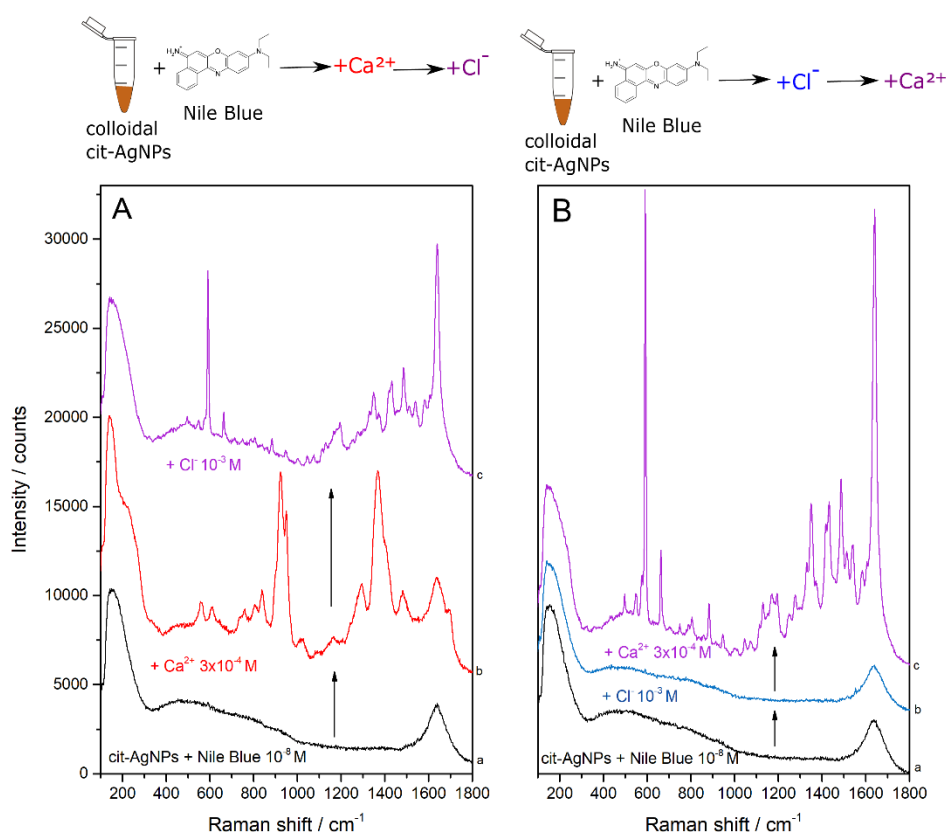


Fig. 4 – SERS spectra of Nile Blue (10^{-8} M) and citrate (10^{-3} M) obtained by tuning the nanoparticle surface potential. (A) (a) Blank spectrum, as the intrinsic electrochemical potential of as-synthesized cit-AgNPs does not support adsorption of either citrate (10^{-3} M) or Nile Blue (10^{-8} M). (b)

Subsequent addition of Ca^{2+} shifts the surface potential toward positive values, switching on the SERS spectrum of anionic citrate. (c) Subsequent addition of Cl^- displaces citrate due to its higher surface affinity, while simultaneously tuning the potential toward negative values, which activates the SERS spectrum of Nile Blue from the mixture. (B) (a) Blank spectrum of Nile Blue (10^{-8} M) in as-synthesized cit-AgNPs. (b) Even after the subsequent addition of Cl^- , no signal is observed, as the intrinsic electrochemical potential of as-synthesized cit-AgNPs does not support Cl^- adsorption. (c)

Addition of Ca^{2+} first tunes the potential toward positive values, followed by Cl^- adsorption that drives the potential negative, ultimately switching on the SERS spectrum of Nile Blue.

Upon addition of Ca^{2+} to cit-AgNPs, the nanoparticle surface undergoes oxidation, which lowers the Fermi level and shifts the electrochemical potential toward more

positive values (schematically illustrated in Fig. 5). This shift favors the adsorption of negatively charged species, as evidenced by citrate binding and the consequent activation of the citrate SERS spectrum (Fig. 4A, spectrum b).

Subsequent addition of Cl^- causes the citrate peaks to vanish and the SERS spectrum of Nile Blue to emerge (Fig. 4A, spectrum c). This behavior can be understood in two steps. First, at positive surface potentials, chloride exhibits stronger binding to silver than citrate, thereby displacing it from the adsorption sites. Second, chloride adsorption alters the electronic structure of the nanoparticle. According to Marichev [12], this involves partial charge transfer from Cl^- to the AgNP surface, while Henglein [13], described a charge redistribution mechanism whereby adsorbed Cl^- creates a surface dipolar layer (δ^+ at surface atoms, δ^- in the particle interior). In both descriptions, chemisorption of chloride induces electron accumulation inside the nanoparticle, raising the Fermi level and shifting the electrochemical potential toward more negative values.

Thus, chloride adsorption simultaneously displaces citrate (Fig. 4A, spectrum c) and elevates the nanoparticle Fermi level (Fig. 5), thereby favoring the adsorption of the cationic analyte Nile Blue and enabling its SERS activation. Together, these effects explain the disappearance of citrate signal and the appearance of the characteristic SERS spectrum of Nile Blue following Cl^- addition.

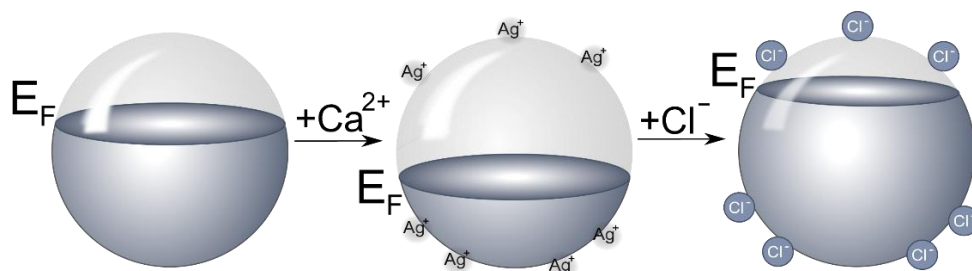


Fig. 5 – Schematic illustration of the behavior of silver nanoparticles (AgNPs) as nanoelectrodes. Ca^{2+} induces surface acidification and lowers the Fermi level through electron depletion and Ag^+ formation. The resulting positive electrochemical potential promotes Cl^- adsorption, followed by partial electron transfer to the nanoparticle, which raises the Fermi level.

The sequence of ion addition - and thus the order of surface-potential modulation - is critical for SERS activation. When Cl^- is added first, no SERS signal is observed for 10^{-8} M Nile Blue in cit-AgNPs (Fig. 4B, spectrum b), because the intrinsic electrochemical potential of the as-synthesized colloid is not sufficiently positive to drive chloride adsorption. Subsequent addition of Ca^{2+} shifts the surface potential toward more positive values, increasing the affinity for anions; competitive adsorption then favors Cl^- over citrate due to its higher surface affinity. Adsorption of Cl^- leads to partial charge transfer to silver, elevating the Fermi level (Fig. 5)

and creating an electrochemical environment favorable for adsorption of the cationic dye Nile Blue. Thus, the cooperative, sequential action of Ca^{2+} and Cl^- tunes the nanoparticle Fermi level in opposite directions, creating surface conditions that enable SERS activation of both anionic and cationic analytes.

The competitive adsorption of anions can be contextualized by the markedly different aqueous solubilities of the corresponding silver salts, as already noted in an early electrochemical SERS study by Pettinger [1]. Silver chloride (AgCl) is sparingly soluble in water, with an intrinsic solubility of $\sim 3 \times 10^{-7}$ M at 25 °C, whereas trisilver citrate is more - though still only modestly - soluble (~ 0.3 g L^{-1} , $\approx 2.8 \times 10^{-3}$ M) under standard conditions. The difference in solubility between AgCl and trisilver citrate explains the stronger adsorption of Cl^- compared to citrate.

Similarly, within complex matrices (e.g., biofluids), the intense SERS signal of uric acid can be rationalized by the extremely low water solubility of deprotonated uric acid (urate) Ag^+ complex [17], which drives the interfacial equilibrium toward adsorbed urate and thereby enhances its SERS response.

The *in situ* modulation of the electrochemical potential of AgNPs by atomic ions, through electron depletion or donation (Fig. 5), governs the selective adsorption of anionic or cationic species onto the nanoparticle surface, followed by their SERS activation. In this sense, metallic nanoparticles behave like nanoelectrodes: their surface electrochemical potential (or Fermi level) determines which charged analytes are preferentially adsorbed. Just as in conventional electrochemistry, where the electrode potential can be tuned externally, here the potential of the nanoparticle surface is tuned by atomic ions. Multivalent cations such as Ca^{2+} reduce the length of the electric double layer and enrich protons at the silver surface, driving the interfacial redox reaction $\text{Ag}^0 \rightarrow \text{Ag}^+ + \text{e}^-$. The resulting depletion of metal electrons increases the work function (corresponding to a downshift of the Fermi level) and shifts the surface potential toward more positive values. This Fermi-level downshift favors adsorption of anionic species such as citrate or chloride. In contrast, halides such as Cl^- elevate the Fermi level via partial charge transfer to the metal surface, shifting the potential toward more negative values and promoting the adsorption of cationic species such as Nile Blue. Thus, colloidal nanoparticles function as nanoscale electrochemical platforms in which atomic ions modulate surface potential and, consequently, analyte adsorption and SERS activity.

4. CONCLUSIONS

This study demonstrates the central role of the nanoparticle surface potential in governing molecular adsorption and the generation of the surface-enhanced Raman scattering (SERS) signal. The electrochemical potential (Fermi level) of the

nanoparticle dictates the selective adsorption of anionic and cationic analytes, positioning them within regions of maximum field intensity and thereby ensuring strong Raman enhancement. Thus, SERS sensitivity and detection limits arise from the interplay between the nanoparticle's optical response, surface potential, and competitive adsorption of analytes.

Importantly, we establish a direct link between selective SERS detection of charged molecules and the nanoparticle Fermi level, showing that adsorption - rather than aggregation - is the dominant factor underlying the selective activation of SERS signals. Since SERS is fundamentally a first-layer effect, only molecules directly adsorbed onto the nanoparticle surface contribute to the spectral response.

The addition of Ca^{2+} to colloidal silver increases ionic strength and shortens the Debye length, suppressing migration and rendering ion transport predominantly diffusion-driven. Because protons diffuse more rapidly than hydroxide ions, this imbalance promotes preferential H^+ accumulation at the nanoparticle interface, inducing local surface acidification. The enriched proton environment facilitates redox interactions with dissolved oxygen, driving silver oxidation, electron depletion, and Ag^+ release. These processes downshift the Fermi level and shift the surface potential toward more positive values, thereby favoring adsorption of anionic species such as citrate or chloride.

Conversely, halide ions such as Cl^- adsorb onto positively charged nanoparticles and shift the surface potential to negative values through partial charge transfer. This inversion of interfacial potential facilitates the adsorption of cationic molecules such as Nile Blue and enables their sensitive SERS detection at concentrations as low as 10^{-8} M.

More broadly, integrating our findings with previous studies, we conclude that nanoparticles behave as nanoelectrodes, with their surface potential dynamically modulated *in situ* by atomic ions. Cations at $\sim 5 \times 10^{-4}$ M (e.g., Ca^{2+} , Mg^{2+} , Pb^{2+} , Al^{3+}) promote electron depletion through Ag^+ formation, thereby lowering the Fermi level. In contrast, halides at $\sim 10^{-3}$ M (Cl^- , Br^- , I^-) partially transfer electrons to the nanoparticle surface, raising the Fermi level and promoting the adsorption of cationic analytes, which in turn enables their SERS activation. This is analogous to shifting the voltage of an electrochemical electrode in the double-layer charging region (i.e., capacitive region) which leads to selective adsorption. Nonetheless, other effects could also drive the selective adsorption of anionic and cationic analytes upon the addition of atomic ions, such as Hoffmeister effects (breaking the surface water layer) or electrostatic interactions between ions and the counter charged analyte. These possible mechanisms must be studied in future studies also on different nanoparticles such as Au instead of Ag.

In brief:

- Three key factors determine the SERS response: the optical properties of the nanoparticles, their surface potential, and the competitive adsorption of analytes.
- The electromagnetic field reaches its maximum intensity at the nanoparticle surface.
- Nanoparticles behave as nanoelectrodes, with their surface potential modulated *in-situ* by atomic ions at sub-millimolar concentrations. The Fermi level of AgNPs shifts downward through electron depletion associated with surface Ag^+ formation, or upward through electron donation from halide ions.
- Anionic analytes preferentially adsorb on surfaces with relatively positive electrochemical potentials, whereas cationic analytes preferentially adsorb on surfaces with relatively negative potentials.
- Molecular adsorption is inherently competitive and governed by the relative affinity of analytes for surfaces characterized by a given electrochemical potential.

ACKNOWLEDGEMENTS

Funding from the Romanian Ministry of Research and Innovation, CCCDI-UEFISCDI, under project numbers PN-IV-P2-2.1-TE-2023-0342 and PN-IV-P2-2.1-TE-2023-0375 is highly acknowledged.

REFERENCES

1. T. Watanabe, O. Kawanami, K. Honda and B. Pettinger, *Evidence for surface Ag^+ complexes as the SERS-active sites on Ag electrodes*, Chemical Physics Letters **102**, 565-570 (1983).
2. C. G. Blatchford, O. Siiman and M. Kerker, *Potential dependence of surface-enhanced Raman scattering from citrate on colloidal silver*, The Journal of Physical Chemistry **87**, 2503-2508 (1983).
3. S. Han, S. Hong and X. Li, *Effects of cations and anions as aggregating agents on SERS detection of cotinine (COT) and trans-3'-hydroxycotinine (3HC)*, Journal of Colloid and Interface Science **410**, 74-80 (2013).
4. A. Otto, A. Bruckbauer and Y. X. Chen, *On the chloride activation in SERS and single molecule SERS*, Journal of Molecular Structure **661-662**, 501-514 (2003).

5. A. M. Chiriac, R. A. Ciceo-Lucacel, S. D. Iancu and N. Leopold, *Citrate-reduced silver nanoparticles: Synthesis temperature dependent properties*, Applied Surface Science **709**, 163759 (2025).
6. A. Stefancu, S. Lee, L. Zhu, M. Liu, R. C. Lucacel, E. Cortés and N. Leopold, *Fermi Level Equilibration at the Metal–Molecule Interface in Plasmonic Systems*, Nano Letters **21**, 6592-6599 (2021).
7. S. D. Iancu, A. Stefancu, V. Moisoiu, L. F. Leopold and N. Leopold, *The role of Ag⁺, Ca²⁺, Pb²⁺ and Al³⁺ adions in the SERS turn-on effect of anionic analytes*, Beilstein Journal of Nanotechnology **10**, 2338-2345 (2019).
8. N. Leopold, A. Stefancu, K. Herman, I. S. Tódor, S. D. Iancu, V. Moisoiu and L. F. Leopold, *The role of adatoms in chloride-activated colloidal silver nanoparticles for surface-enhanced Raman scattering enhancement*, Beilstein Journal of Nanotechnology **9**, 2236-2247 (2018).
9. A. Stefancu, S. D. Iancu, V. Moisoiu and N. Leopold, *Specific and selective SERS active sites generation on silver nanoparticles by cationic and anionic adatoms*, Romanian Reports in Physics **70**, (2018).
10. A. Stefancu, S. D. Iancu and N. Leopold, *Selective Single Molecule SERRS of Cationic and Anionic Dyes by Cl⁻ and Mg²⁺ Adions: An Old New Idea*, The Journal of Physical Chemistry C **125**, 12802-12810 (2021).
11. S. D. Iancu, V. Moisoiu, B. A. Tigu, A. Stefancu, O. M. Biro, C. Tomuleasa and N. Leopold, *SERS-based detection of DNA methylation for cancer diagnosis: Cation-mediated adsorption to silver nanoparticles*, PLOS ONE **20**, e0325539 (2025).
12. V. A. Marichev, *First experimental evaluation of partial charge transfer during anion adsorption*, Colloids and Surfaces A: Physicochemical and Engineering Aspects **348**, 28-34 (2009).
13. P. Mulvaney, T. Linnert and A. Henglein, *Surface chemistry of colloidal silver in aqueous solution: observations on chemisorption and reactivity*, The Journal of Physical Chemistry **95**, 7843-7846 (1991).
14. P. C. Lee and D. Meisel, *Adsorption and surface-enhanced Raman of dyes on silver and gold sols*, The Journal of Physical Chemistry **86**, 3391-3395 (1982).
15. T. Stepan, L. Tété, L. Laundry-Mottiar, E. Romanovskaia, Y. S. Hedberg, H. Danninger and M. Auinger, *Effect of nanoparticle size on the near-surface pH-distribution in aqueous and carbonate buffered solutions*, Electrochimica Acta **409**, 139923 (2022).
16. M. D. P. Souza, G. Moro, R. S. Melo, L. M. Moretto, S. L. D. C. Brasil and C. Zanardi, *Carbon steel corrosion monitoring: Why opting for an electroanalytical approach*, Journal of Electroanalytical Chemistry **995**, 119312 (2025).
17. C. A. MacMunn, *Outlines of the Clinical Chemistry of Urine*, Churchill, London, 1889, page 68.